

AFRICON 2004 POWER SPECIAL ISSUE

SWITCHED RELUCTANCE MOTOR MEASUREMENTS AND SIMULATION MODELS

Sen Wang*, Bruce Burton** and R.G. Harley***

** School of Electrical and Electronic Engineering, University of KwaZulu-Natal, King George V Ave, Durban, 4041, South Africa*

*** School of Electrical and Electronic Engineering, University of KwaZulu-Natal, King George V Ave, Durban, 4041, South Africa*

**** School of Electrical and Electronic Engineering, University of KwaZulu-Natal, King George V Ave, Durban, 4041, South Africa*

Abstract: This Paper describes an experimental process used to produce a model in Matlab and Simulink for a prototype 8/6 Switched Reluctance Motor, and some methods used to validate the model. The inductance, flux and torque characteristics of switched reluctance motors are nonlinear, and must usually be numerically determined from real experimental data. Torque can be measured directly or calculated from measured phase current and rotor position, and numerically determined inductance. This paper explains how two different lookup tables are used to simulate the electrical, magnetic and mechanical characteristics of the motor. Simulation results are shown to closely agree with practical current and rotor position responses under locked and free rotor conditions. It is also explained how the validated simulation models will be used in the future design of a power converter and nonlinear torque (current) and speed control loops.

Key words: Switched reluctance motor, simulation model, measurements.

1. INTRODUCTION

The simple structure and principle of operation make switched reluctance motor (SRM) very different from other types of motors. This paper considers a four phase SRM with 8 stator poles (s1, s2, s3, s4, s1', s2', s3', s4') and 6 rotor poles (A to G), as shown in Figure 1(a). In this motor, the four stator phases are created by connecting opposite stator coil pairs in series (s1-s1', s2-s2', s3-s3', s4-s4') so that they are energised simultaneously. When the two poles of a stator phase are energised, the nearest two rotor poles will experience a torque which will tend to move them to a position in which they completely overlap with the energised stator poles (the aligned position for that phase). This torque occurs because the reluctance of the magnetic circuit decreases as the overlap between the energised stator poles and nearest rotor poles increases. The rotor can therefore be made to rotate in either direction by sequentially energizing consecutive stator phases [1-2]. Positive rotation is defined in the anti-clockwise direction. The rotor position is defined from 0° to 360°, as shown in Figure 1(a), irrespective of direction.

In Figure 1(a), rotor pole pairs A-D and C-F are completely unaligned with phase s1-s1'. Energising only s1-s1' in this position will produce no net torque, as the two adjacent rotor pole pairs will both be equally attracted to the energised s1 poles. Each stator phase, however, is usually only energised when a rotor pole is

unaligned by 15° or less for an 8/6 SRM [3]. In Figure 1(b), for example, rotor pole pair A-D is aligned with s1-s1'. Energising only s2-s2' in this position can move the rotor through 15° to align rotor pole pair B-E with s2-s2'. Subsequent individual energization of s3-s3' and then s4-s4' can therefore move the rotor through a further 15° each. One stator cycle is defined as one such sequence of individual energization of the four phases, and can therefore only move the rotor through $4 \times 15^\circ = 60^\circ$. Six stator cycles are therefore required to move the rotor of an 8/6 SRM through one complete revolution (360°). The rotor position is defined to be 0° when the rotor pole pair A-D is aligned with s1-s1' showed in Figure 1. The next section develops mathematical models for numerical simulation of SRMs.

2. MATHEMATICAL SRM MODELS

SRM models are generally made up of three parts: the electrical model, torque characteristic, and mechanical model. This section develops the first two of these models. A simple mechanical model is presented in section 3. The electrical circuit for one phase of SRM is shown in Figure 2. Applying Kirchhoff voltage law (and omitting time dependencies (t) for simplicity) gives

$$v = iR + \frac{d\lambda(\theta, i)}{dt} \quad (1)$$

Where R is the phase resistance (assumed to be constant).

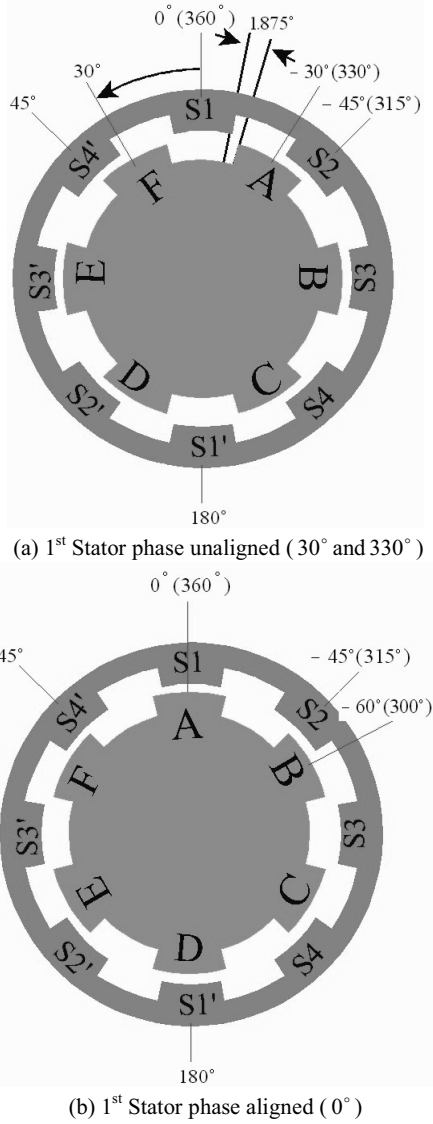


Figure 1: Cross section of an 8/6 SRM

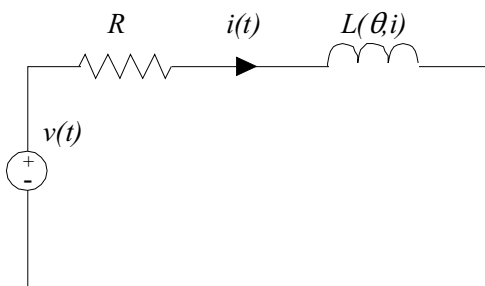


Figure 2: Equivalent circuit for one stator phase

Magnetic flux $\lambda(\theta, i)$ is given by

$$\lambda(\theta, i) = L(\theta, i)i \tag{2}$$

Where $L(\theta, i)$ is the phase inductance, which varies as a function of rotor position (due to varying reluctance) and phase current (due to magnetic saturation).

Equation (1) can be solved to calculate the magnetic flux at various rotor angles and current magnitudes from measured stator voltages, currents and resistance as shown in (3).

$$\lambda(\theta, i) = \int (v - iR) dt \tag{3}$$

A lookup table can then be constructed to determine the per phase values of inductance for various rotor angles and current magnitudes using (4) (as shown in section 3).

$$L(\theta, i) = \frac{\lambda(\theta, i)}{i} \tag{4}$$

The current response to a particular voltage input can be then be simulated using (5), as shown in section 4.

$$i = \frac{\int (v - iR) dt}{L(\theta, i)} \tag{5}$$

The electrical model of the SRM can be compared with that of a DC motor by substituting (2) into (1) as follows.

$$\begin{aligned} v &= iR + \frac{d(L(\theta, i)i)}{dt} \\ &= iR + L(\theta, i) \frac{di}{dt} + i \frac{d(L(\theta, i))}{dt} \end{aligned} \tag{6}$$

$$\begin{aligned} &= iR + L(\theta, i) \frac{di}{dt} + i \frac{d\theta}{dt} \frac{d(L(\theta, i))}{d\theta} \\ &= iR + L(\theta, i) \frac{di}{dt} + i\omega \frac{d(L(\theta, i))}{d\theta} \end{aligned} \tag{7}$$

The mechanical rotor speed is $\omega = \frac{d\theta}{dt}$. The term $i\omega \frac{d(L(\theta, i))}{d\theta}$ in (7) is analogous to the armature back emf in DC motors[4], and shows that higher supply voltage is required to achieve higher rotor speed.

The remainder of this section shows how the more complex SRM torque characteristic can be derived from the nonlinear phase inductance characteristic. Figure 3 shows an idealised curve of s1-s1' phase inductance vs rotor position for the 8/6 SRM in Figure 1.

In this curve, L_a is phase inductance at the A-D rotor pair aligned position (0°) and L_{un} is phase inductance at the two completely unaligned positions (30° and 330°). This curve is symmetrical about the aligned position. The s1-s1' stator poles and A-D rotor poles completely overlap each other for rotor angles from 358.75° to 1.25° . The idealized inductance then begins to decrease as the amount of overlap decreases to zero in both directions. The constant minimum idealized inductance L_{un} is reached for zero overlap on each side of the stator pole (outside of $[331.875^\circ, 28.125^\circ]$).

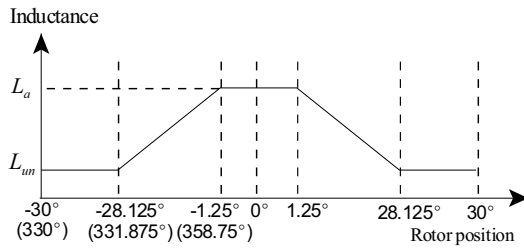


Figure 3: Idealised curve of s1-s1' phase inductance vs rotor position for one value of phase current in an 8/6 SRM

Figure 4 shows the power flow through a SRM.

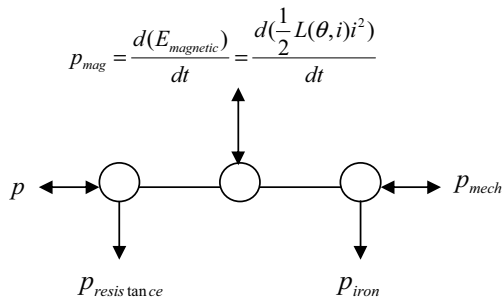


Figure 4: SRM power flow diagram

In motor mode, the electrical input power p is equal to the sum of: (i) resistance loss $P_{resistance}$, (ii) iron loss P_{iron} , (iii) rate of change of stored magnetic energy P_{mag} , and (iv) mechanical output power P_{mech} .

Idealised/measured inductance vs position curves for various current values can be used to determine corresponding idealised/measured torque curves by assuming negligible iron losses and equating instantaneous air gap power to mechanical output power. The instantaneous electrical input power for each stator

phase is given by the product of instantaneous voltage and current.

$$p = iv \quad (8)$$

$$p = Ri^2 + i^2 \frac{dL(\theta, i)}{dt} + L(\theta, i)i \frac{di}{dt} \quad (9)$$

The first term in (9) is $P_{resistance}$. The second and third terms therefore represent the sum of P_{mag} and the P_{mech} (assuming negligible iron losses). The contribution of the second and third terms to P_{mag} and P_{mech} can therefore be determined from the definition of P_{mag} [3].

$$\begin{aligned} P_{mag} &= \frac{d}{dt} \left(\frac{1}{2} L(\theta, i) i^2 \right) \\ &= L(\theta, i) i \frac{di}{dt} + \frac{1}{2} i^2 \frac{dL(\theta, i)}{dt} \end{aligned} \quad (10)$$

Substituting (10) into (9) gives

$$p = Ri^2 + \frac{d}{dt} \left(\frac{1}{2} L(\theta, i) i^2 \right) + \frac{1}{2} i^2 \frac{dL(\theta, i)}{dt} \quad (11)$$

The second term in (11) is therefore P_{mag} , and the third term is P_{mech} , which is also equal to the product of torque and rotor speed, i.e.

$$\frac{1}{2} i^2 \frac{dL(\theta, i)}{dt} = T(\theta, i) \omega \quad (12)$$

where $\omega = \frac{d\theta}{dt}$. The instantaneous torque is therefore given in terms of instantaneous current and rate of change of inductance with rotor position, as shown in (13).

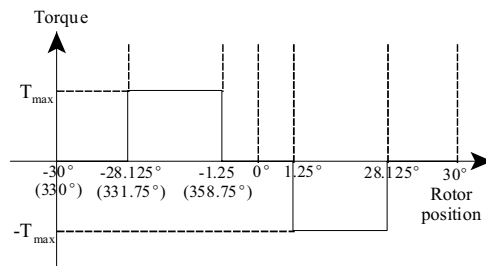


Figure 5: Idealised curve of s1-s1' phase torque vs rotor position for one value of phase current in an 8/6 SRM

$$\begin{aligned} T(\theta, i) &= \frac{1}{2} i^2 \frac{dL(\theta, i)}{dt} \frac{dt}{d\theta} \\ &= \frac{1}{2} i^2 \frac{dL(\theta, i)}{d\theta} \end{aligned} \quad (13)$$

Figure 5 shows the idealised torque curve corresponding to the idealised inductance curve in Figure 3. Positive/negative torque is produced when inductance increases/decreases with increasing position. Zero torque is produced in positions where inductance does not vary with varying position. From Figure 5, it can be seen that positive/negative torque can be produced through nearly 30° , but it has been explained in section one that only 15° of this curve can be used if only one stator phase is energised at a time. The next section derives real phase inductance curves and corresponding torque curves from stator voltage and current measurements.

3. PHASE INDUCTANCE AND TORQUE MEASUREMENTS

Figure 6 shows a block diagram of the experimental setup used to make all of the practical SRM measurements presented in this paper.

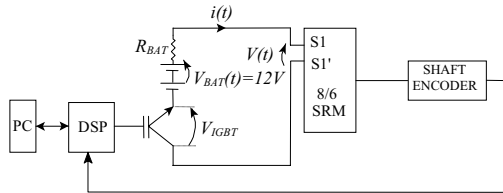


Figure 6: Block diagram of SRM measurement setup

Figure 7 shows 31 measured voltage and current curves obtained by switching a 12v battery across the terminals of the series s1-s1' circuit with the rotor locked in steps of 1° from 0° to 30° . The stator terminal voltage drops with increasing current due to the internal battery resistance, cable resistance and forward IGBT voltage characteristic.

Figure 8 shows graphs of flux vs current for each locked rotor position in Figure 7. These graphs were calculated by substituting corresponding graphs of voltage and current into (3).

Figure 9 shows graphs of s1-s1' phase inductance vs rotor position for various values of phase current. These graphs were obtained by substituting regularly interpolated current and flux values from the graphs of Figure 8 into (4).

Figure 10 shows graphs of s1-s1' phase torque vs rotor position for various values of phase current. These graphs were obtained by substituting phase current and inductance gradient with respect to rotor positions from the graphs of Figure 9 into (13) to achieve the torque characteristic.

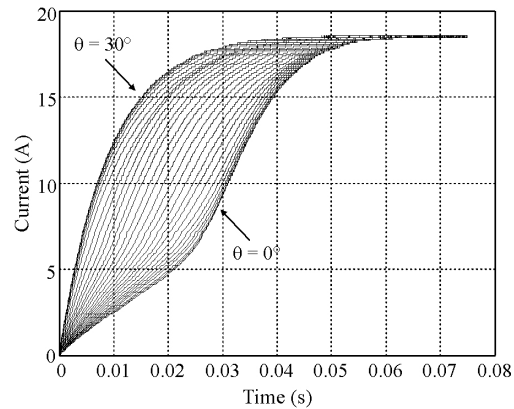
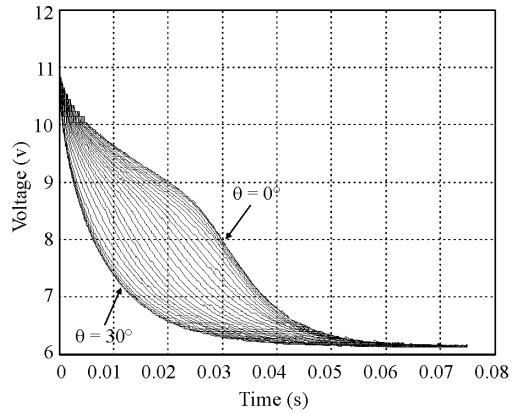


Figure 7: Measured phase voltage and current with rotor is locked at fixed angles $\theta \in \{0^\circ, 1^\circ, 2^\circ, \dots, 30^\circ\}$

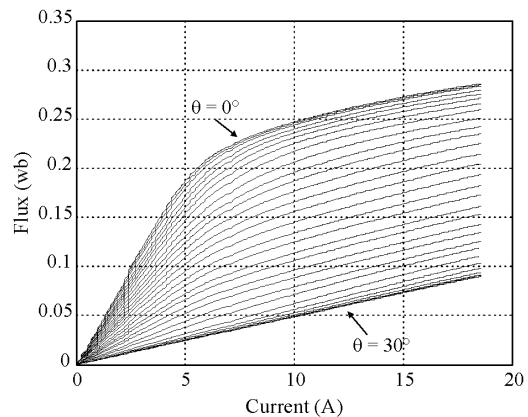


Figure 8: Flux vs current for different locked rotor positions $\theta \in \{0^\circ, 1^\circ, 2^\circ, \dots, 30^\circ\}$

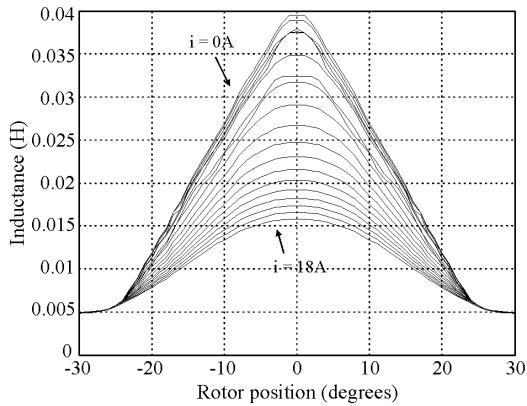


Figure 9: Phase inductance vs rotor position for different current magnitudes

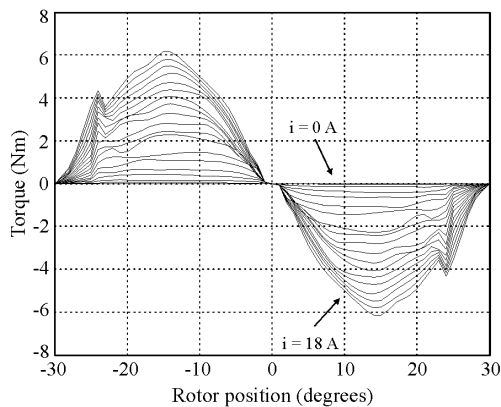


Figure 10: Torque characteristic vs rotor position for different current magnitudes

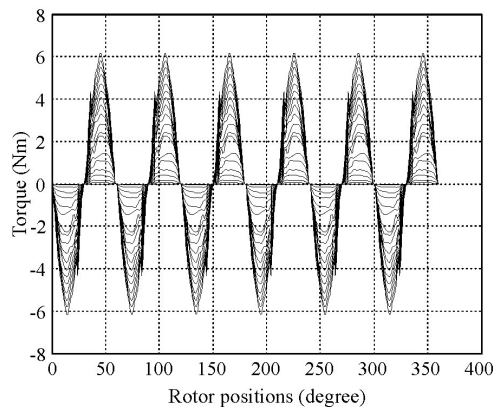


Figure 11: Periodic torque of 1st stator phase vs rotor position from 0° to 360° for different fixed current values

It can be seen from Fig. 1 that the inductance variations caused in $s1-s1'$ by (i) the A-D rotor pole pair as the rotor

moves from 330° to 30° will be repeated by: (ii) B-E from 30° to 90°, (iii) C-F from 90° to 150°, (iv) D-A from 150° to 210°, (v) E-B from 210° to 270°, and (vi) F-C from 270° to 330°. Fig. 11 shows the corresponding periodic torque which would result if the current were held at various fixed values while the rotor was moved through 360°.

The next section develops simlink models from the measured phase inductance and derived torque characteristics, and compares simulated and measured locked and free rotor responses.

4. SIMULATION AND MEASURED RESULT

Figure 12 shows a Simulink implementation of the electrical model presented in section 2. Equation (5) is used to obtain the locked rotor current response to a particular terminal voltage curve. The inductance curves in Figure 9 are incorporated in the form of a 2-D lookup table with current and position indices.

Figure 13 compares simulated and measured current responses for a locked rotor position of 5° (similar results were produced at other rotor angles). The measured terminal voltage was used in the simulation to account for the voltage drops in the practical system, as observed in Figure 7.

The close agreement between the measured and simulated current responses confirms the validity of the mathematical and simulation models of each stator circuit under locked rotor conditions.

Free rotor simulations require the inclusion of model to determine the mechanical position and speed responses to the torque produced by the SRM. In this paper, the SRM was not connected to any other mechanical system (apart from the rotor locking mechanism, which was removed during free rotor tests). The first order model in (14) could therefore be used as shown in Figure 14 to account for the SRMs own inertia and viscous friction.

$$T = J \frac{d\omega}{dt} + B\omega \quad (14)$$

Figure 15 shows how the electrical model of Figure 12 was combined with the torque characteristic of Figure 10 and the mechanical model of Figure 14 to simulate the free rotor response when a 12V battery was switched across the terminals of the series $s1-s1'$ circuit. The torque characteristic is entered in the form of a 2-D lookup table with current and position indices. The range of the angle index is limited to $[330^\circ, 30^\circ]$ $[-30^\circ, 30^\circ]$, because the rotor position is not expected to exceed this range for initial rotor positions inside it. The initial rotor position

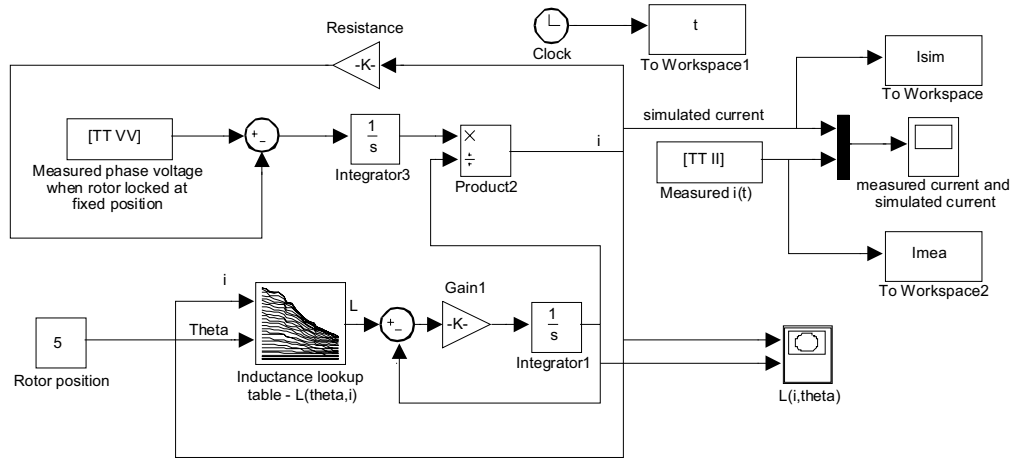


Figure 12: Electrical model for each SRM stator phase with locked rotor

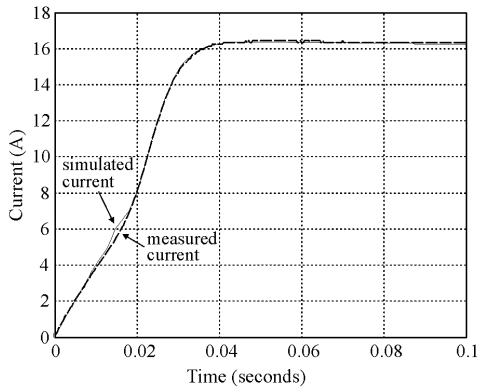


Figure 13: Simulated and measured current responses for a locked rotor position of 5°

is entered (in radians) in the form of an initial condition on integrator2 in Figure 14.

Figure 16 compares simulated and measured current and rotor position responses when the rotor is free to move from an initial position of 15°. The measured voltage across the phase s1-s1' is also used as the input voltage in this simulation.

Figure 16 shows that the simulated phase current and rotor position response closely agree with measured current and rotor angle. The results prove that the torque characteristics and mechanical model for the one phase SRM simulation model are working well. In addition, the electrical model is also shown to be valid under free rotor conditions, and all three models have been correctly combined to simulate one phase of the whole SRM.

The next section discusses the simulation of the complete 8/6 SRM by combining four one phase models, and various strategies for torque control.

5. FOUR PHASE SIMULATION MODEL AND TORQUE CONTROL STRATEGIES FOR 8/6 SRM

Figure 17 shows the four phase individually energized model for an 8/6 SRM. A constant current source is sequentially switched into one phase circuit at a time. A current source is chosen in this hypothetical model to illustrate the need for current control to implement any effective torque control strategy. The initial rotor angle is set to 345°, as explained in section 1. Each complete rotor revolution is then produced by commutating the current source from one phase to the next at the end of each corresponding 15° change in rotor angle. One complete rotor revolution therefore requires six stator cycles. Figure 18 shows the simulated torque and speed responses produced by this hypothetical strategy.

Replacement of the ideal current source commutation scheme in Figure 17 with a practical current controlled voltage source will result in a more discontinuous torque response than that seen in Figure 18(a), due to practical limitations on the current rise and fall times. A completely different approach is therefore required to achieve near constant instantaneous torque responses.

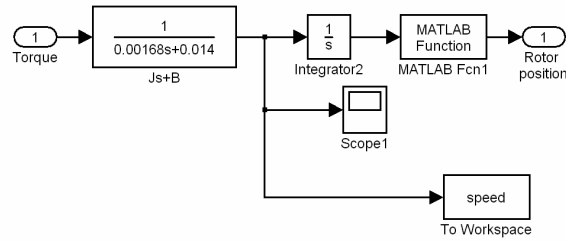


Figure 14: Mechanical shaft model

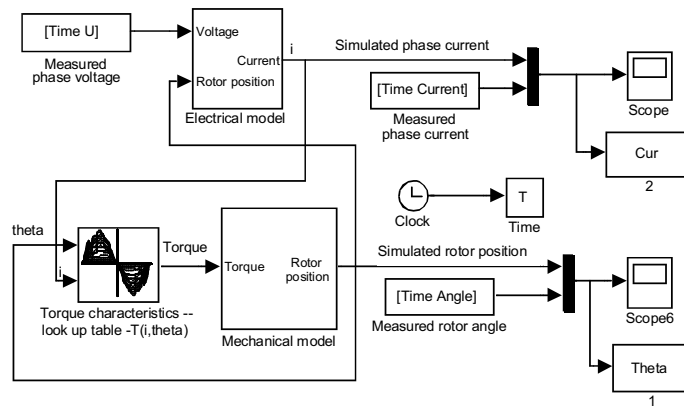
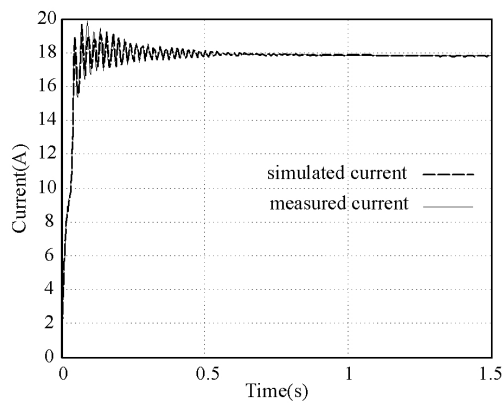
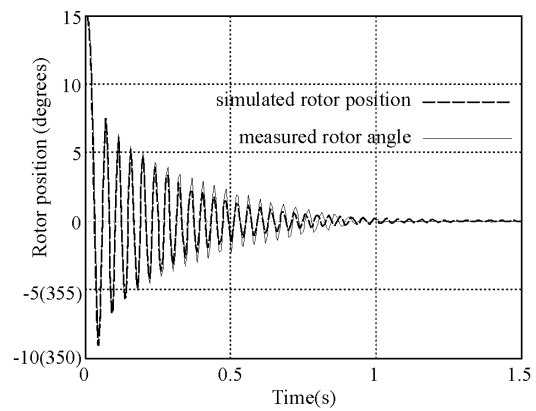


Figure 15: One phase SRM simulation model with free rotor



(a) Measured and simulated current curve



(b) Measured and simulated rotor position curve

Figure 16: Free rotor test results when rotor starts from 15°

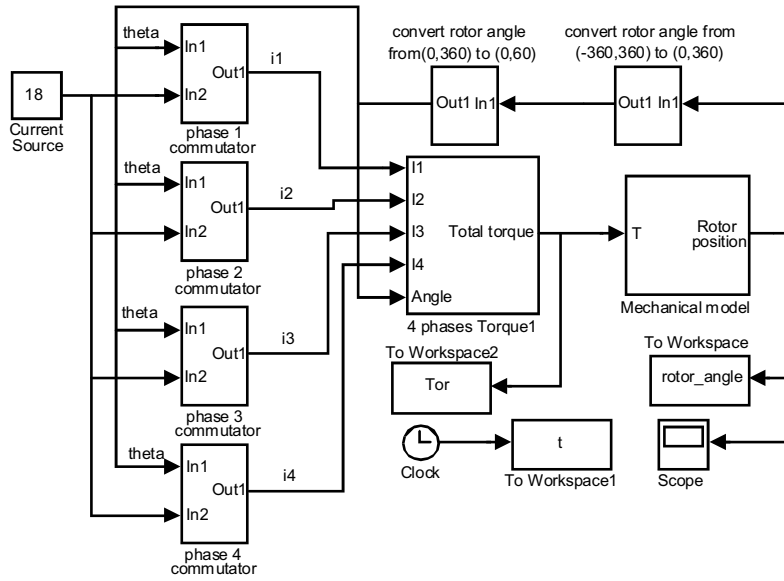


Figure 17: Four phase simulation model for an 8/6 SRM with commutated current source

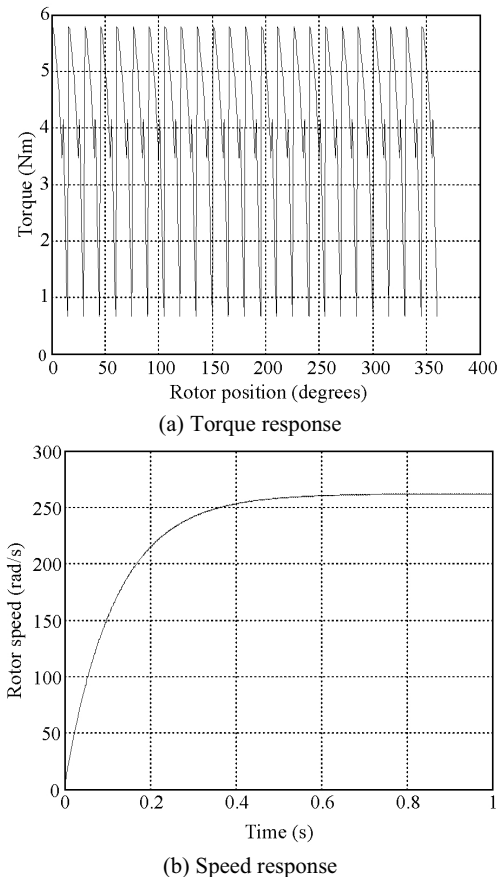


Figure 18: Torque and speed responses produced by simulation of ideal current source commutation

Subplots (a) to (d) in Figure 19 show the torque which can be produced in each rotor position for various values of current in each of the four phases of the 8/6 SRM. Any two of these four sets of torque curves can be added together in only 6 unique ways. Subplot (e) shows the 6 combined torque curves for maximum current (18A). Combining more than two phase torques at a time would serve no practical purpose as only two phase torques will have the same sign for any given rotor angle. It can be seen that two of these combinations (phase 1 plus 3, and phase 2 plus 4) produce near zero torque, but the other four combinations produce torques which (i) have a higher peak magnitude than each phase torque, but (more importantly) (ii) overlap with each other. This means any constant or time varying torque value (inside the envelope defined by these four curves) can be achieved by forcing any appropriate combination of currents to flow in the appropriate two phases for a given instantaneous rotor angle.

Practical implementation of this bi-phase torque control strategy for four phase SRMs (such as the 8/6 motor considered in this paper) will require the development of (i) algorithms to determine appropriate instantaneous current values for all four phases, and (ii) converter hardware and current control algorithms to track the resulting current trajectories. Future work will focus on the design and implementation of (i) a suitable power converter, (ii) a simple current reference generator, and (iii) a nonlinear current controller. Further work will also focus on optimal current reference generation and speed control.

6. CONCLUSIONS

A step-by-step introduction and theoretical analysis of an 8/6 SRM have been presented. Actual inductance and torque characteristics have been derived from measured locked rotor phase voltage and current responses. A simulation model for this motor has been proposed and tested under locked and free rotor conditions. The validity of this model has been established by closely matching simulation and measured responses under both of these conditions. The use of this model in future work on the development of current and torque control algorithms and hardware has also been discussed.

7. REFERENCES

[1] Buja GS and Valla MI, "Control Characteristics of Switched-Reluctance Motor Drives", *Proceedings of the IEEE International Workshop on Intelligent*

Motion Control, Vol 2, pp. 675 – 682, 20-22 August 1990.

[2] Torrey D A and Lang J H , "Modeling a nonlinear variable-reluctance motor drive", *IEE Proceedings on Electric Power Applications*, Vol 137, pp. 314-326 Sep 1990.

[3] Ramu. Krishnan: *Switched Reluctance Motor Drives: Modelling, Simulation, Analysis, Design and Applications*, CRC press, Florida, USA, pp.7-21, 2001.

[4] Cui P, Zhu JG, Ha QP, Hunter GP and Ramsden VS, "Simulation of nonlinear switched reluctance motor drives with PSIM", *Proceedings of the Fifth International Conference on Electrical Machines and Systems*, Shenyang, China, Vol 2, pp.1061 – 1064, 18-20 Aug. 2001.

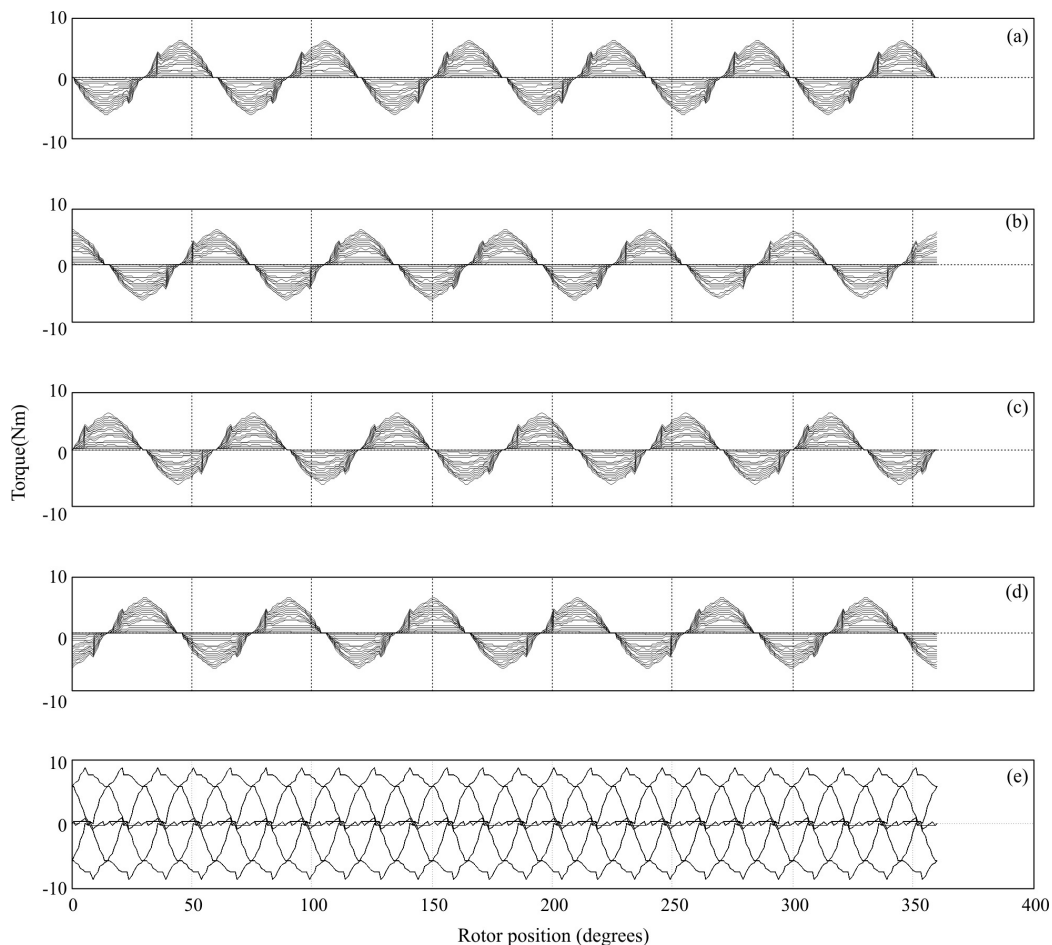


Figure 19 (a) – (d): Four phase torques vs rotor angle for various fixed current magnitudes and (e) sum of maximum torque curves for all six unique phase pairs